Biochimica et Biophysica Acta 891 (1987) 157–164
Elsevier

BBA 42515

Model studies to low-temperature optical transitions of photosynthetic reaction centers. II. *Rhodobacter sphaeroides* and *Chloroflexus aurantiacus*

P.O.J. Scherer and S.F. Fischer

Fachbereich Physik, Technische Universität München, Garching (F.R.G.)

(Received 22 September 1986)

Key words: Optical spectra simulation; Reaction center; Exciton model; Special-pair triplet state; (*Rb. sphaeroides, C. aurantiacus*)

The analysis of optical spectra for *Rhodopseudomonas viridis* from part I (Knapp, E.W., Scherer, P.O.J. and Fischer, S.F. (1986) Biochim. Biophys. Acta 852, 295–305) is extended to two other structurally similar reaction centers with different prosthetic groups (*Rhodobacter sphaeroides* and *Chloroflexus aurantiacus*). Assuming that the structure of the different reaction centers is similar, the interactions between the six prosthetic groups are calculated using the structure data from *Rps. viridis*. The absorbance, linear dichroism (LD), circular dichroism (CD), triplet-minus-singlet absorption-detected magnetic resonance (T – S ADMR) and its linear dichroism are simulated by an exciton model. The results point to partial delocalization of the special pair triplet state and its excitations.

Introduction

In part I [1] we analyzed optical spectra from reaction centers of *Rhodopseudomonas viridis* for which the structural arrangement of the pigments has been determined recently [2]. We showed that different kinds of spectra, including absorbance, linear and circular dichroism as well as triplet-minus-singlet ADMR difference spectra can be understood within an exciton model.

Assuming that the structure of other reaction centers is similar to that of *Rps. viridis*, our exciton model can be applied to investigate their optical spectra. In this paper we concentrate on reaction centers of *Rhodobacter sphaeroides* and *Chloroflexus aurantiacus*. The prosthetic groups of these reaction centers are different from those of *Rps. viridis*. Firstly reaction centers of *Rb. sphaeroides* and *C. aurantiacus* contain BChl *a* and BPheo *a* molecules, whereas *Rps. viridis* contains the *b*-types. Secondly, for *C. aurantiacus* one of the accessory monomers is a pheophytin molecule [3] which differs energetically from the corresponding chlorophyll molecule in the reaction centers of *Rps. viridis* and *Rb. sphaeroides*. A preliminary analysis of the spectra of *C. aurantiacus* by H. Vasmel et al. has been made available to us [4]. Part of their results were published after this paper had been submitted [5]. Our results are consistent with the proposal of Vasmel et al. that the extra pheophytin molecule is located on the M-branch and that its orientation is similar to that of the replaced bacteriochlorophyll.

In part I we also investigated triplet states of the special-pair dimer. We introduced excited triplet states into the exciton model which are de-

Abbreviations: ADMR, absorption-detected magnetic resonance; LD, linear dichroism; CD, circular dichroism; BChl, bacteriochlorophyll; BPheo, bacteriopheophytin.

Correspondence: S.F. Fischer, Fachbereich Physik, Technische Universität München, James-Franck-Strasse, D-8046 Garching, F.R.G.

localized over the special-pair pigments. It is interesting to apply this model to other reaction centers where the degree of triplet delocalization may be different.

General aspects

The model has been described in detail in part I. We consider an arrangement of six pigments (i.e., the special-pair pigments denoted by BC_{MP} and BC_{LP}, the accessory monomers BC_{MA} and BC_{LA} and the pheophytins BP_M and BP_L; for more details see Fig. 1 in Ref. 1), which are coupled via transition-dipole interaction. The coupling constants are calculated using the structure data from *Rps. viridis* and transition dipole squares of $37D^2$ and $23D^2$ for BChl *a* and BPheo *a* molecules respectively. These values are smaller than the $45D^2$ and $30D^2$ we used for *Rps. viridis*, since there is evidence that the transition dipole moments are larger for the *b*-type molecules [6]. The coupling of the special pair pigments which may contain an unknown contribution from exchange interaction and the diagonal energies are treated as free parameters of the model and adjusted to fit the experimental data. The resulting Hamiltonian matrix (Tables I and II) is diagonalized and the intensities of the absorption, LD and CD spectra are calculated.

The T − S ADMR difference spectrum is calculated as the difference of the absorption spectrum of reaction centers in the lowest singlet state and the absorption spectrum of reaction centers in the lowest triplet state. We assume that the triplet excitation is confined to the special pair pigments BC_{MP} and BC_{LP} and use a simplified description of the lowest triplet state T [7,8]

$$T = A\,BC^T_{MP}BC_{LP} + B\,BC_{MP}BC^T_{LP} + C_1\,BC^+_{MP}BC^-_{LP} + C_2\,BC^-_{MP}BC^+_{LP} \quad (1)$$

which allows for delocalization of the triplet over the special-pair pigments as well as for charge-resonance contributions. From a comparison of monomer and dimer *D*-values it can be concluded that the contribution of charge-separated states $C_1^2 + C_2^2$ is between 10% and 30% [8]. The absorption spectrum of reaction centers in the state T is evaluated within a similar exciton model. We consider four states where the special pair is in the triplet state T and one of the accessory monomers or of the pheophytins carries the singlet excitation and two excited triplet states of the special pair T(+) and T(−) which are combinations of states where the triplet is on one special-pair pigment and the singlet excitation on the other.

$$T(+) = \alpha BC^T_{MP}BC^*_{LP} + \beta BC^*_{MP}BC^T_{LP}$$

$$T(-) = -\beta BC^T_{MP}BC^*_{LP} + \alpha BC^*_{MP}BC^T_{LP} \quad (2)$$

We neglect admixtures of charge-separated states as well as higher triplet states, since such states do not contribute significant absorption in the frequency region of the Q_y transitions.

In this approximation transitions from T to T(±) carry the transition dipoles

$$\mu(+) = A\alpha\mu_{LP} + B\beta\mu_{MP}$$

$$\mu(-) = -A\beta\mu_{LP} + B\alpha\mu_{MP} \quad (3)$$

The energy positions of the states T(±) enter as

TABLE I

SINGLET INTERACTIONS AND DIAGONAL ENERGIES FOR *RHODOBACTER SPHAEROIDES*

All values are given in units of cm^{-1}. Diagonal energies are relative to 12500 cm^{-1}, Values in brackets are for simulation of spectra at approx. 80 K.

	BC_{MA}	BC_{LP}	BC_{MP}	BC_{LA}	BP_M	BP_L
BC_{MA}	−30	−146	−38	22	133	−9
BC_{LP}	−146	−630 (−530)	680 (600)	−50	26	−7
$BC_{MP'}$	−38	680 (600)	−630 (−530)	−165	−8	30
BC_{LA}	22	−50	−165	−30	−8	137
BP_M	133	26	−8	−8	700	5
BP_L	−9	−7	30	137	5	570

TABLE II

SINGLET INTERACTIONS AND DIAGONAL ENERGIES FOR *CHLOROFLEXUS AURANTIACUS*

All values are given in units of cm^{-1}. Diagonal energies are relative to 12500 cm^{-1}.

	BP_{MA}	BC_{LP}	BC_{MP}	BC_{LA}	BP_{M}	BP_{L}
BP_{MA}	760	−111	−75	13	113	−6
BC_{LP}	−111	−500	680	−50	26	−7
BC_{MP}	−75	680	−500	−165	−8	30
BC_{LA}	13	−50	−165	−90	−8	137
BP_{M}	113	26	−8	−8	880	5
BP_{L}	−6	−7	30	137	5	820

additional parameters. The energies of the triplet states with singlet excitation on accessory monomers or pheophytins are approximately that of the corresponding singlet states. The expression $(A^2 - B^2)/(A^2 + B^2)$ is a convenient measure of the triplet exciton localization. It is +1 (−1) if the triplet excitation is located on the M-branch (L-branch) and vanishes in case of delocalization.

TABLE III

TRIPLET PARAMETERS

The transition dipole moments of the excited triplet states are calculated according to Eqn. 3. From that, interactions V_{ij} with accessory monomers and pheophytins are calculated via a transition-dipole coupling model. The diagonal energies E_i of the states T(±) are free parameters. All values in Table III are given in cm^{-1}. Energies of T(±) are relative to 12500 cm^{-1}. B*X*MA = BCMA for *Rb. sphaeroides* and BPMA for *C. aurantiacus*.

Triplet properties	*Rb. sphaeroides*	*C. aurantiacus*
CT contribution to T	20%	12%
Localisation of T $\frac{A^2 - B^2}{A^2 + B^2}$	0.4	0.9
Localisation of T(±) $\alpha^2 - \beta^2$	0.5	−0.3
$V_{T(+),BXMA}$	−103	−72
$V_{T(+),BCLA}$	−73	−52
$V_{T(+),BPM}$	15	13
$V_{T(+),BPL}$	3	1
$V_{T(-),BXMA}$	−38	−73
$V_{T(-),BCLA}$	52	−18
$V_{T(-),BPM}$	13	19
$V_{T(-),BPL}$	−15	−8
$E_{T(+)}$	−190	−130
$E_{T(-)}$	420	430

The chosen values of the triplet state parameters are given in Table III.

Finally, suitable line profiles are introduced to provide continuous spectra which can be compared with the experimental data. Each line profile is a sum of three Gaussian functions. Two of them simulate the vibrationless transition and a phonon sideband in the regime of 300 cm^{-1}. Their respective widths (full width at half height, FWHH) are 160 cm^{-1} and 670 cm^{-1} and their intensity ratio is 0.85 : 0.15 for *C. aurantiacus* and 0.75 : 0.25 for *Rb. sphaeroides*. These values are motivated by the spectrum of the isolated chlorophyll molecule and adjusted to account for inhomogeneities [1]. For the lower dimer band the widths are increased to 380 cm^{-1} and 1200 cm^{-1}, and for the *Rb. sphaeroides* intensity ratio is changed to 0.60 : 0.40. A third Gaussian function is added to each line profile which represents intermolecular vibrations around 1350 cm^{-1}. It carries 11% of the intensity of the line profile and has a width of 500 cm^{-1}. For the spectra of the *Rb. sphaeroides* at 80 K the linewidths had to be increased by approx. 60%.

The 1350 cm^{-1} vibration of the lower dimer state overlaps with the accessory monomer absorption. Upon oxidation or optical excitation it is instantaneously bleached together with the special pair band. This should be kept in mind when time-dependent bleaching to electron transfer via the accessory monomer is discussed [9].

Results for *Rhodobacter sphaeroides*

A simulation of the room-temperature absorption spectrum has been presented elsewhere [8].

For the low-temperature spectra we have to increase the dimer coupling by some 100 cm^{-1} and to readjust the diagonal energies. Since the upper dimer band does not show up in the spectra as a distinct feature, the uncertainty in the value of the dimer coupling is quite large. In the following we assume a value of 680 cm^{-1} at 4 K and of 600 cm^{-1} at 80 K. The model spectra, however, are quite similar for dimer couplings in the range of 600–800 cm^{-1} if other free parameters are adjusted properly.

The resulting absorption, CD and LD spectra agree very well with experimental data taken at approx. 80 K [10,11] as shown in Figs. 1–3. For the LD spectrum which was measured on a stretched polymer film we took as the polarization axis the vector (−0.73, 0.49, 0.40) in the crystallographic coordinate system. This vector makes an angle of 76° with the C_2-symmetry axis.

For the simulation of triplet-minus-singlet absorbance difference spectra which were taken at the lower temperature 4 K, the position of the lower dimer band had to be adjusted differently (see Table I). The calculated absorption spectrum for this set of parameters agrees very well with experiments from Breton [12] (not shown).

In the simulated triplet-minus-singlet absorbance difference spectrum (Fig. 4) the triplet states T(+) and T(−) are located at 820 nm and 776 nm, respectively. The symmetric state T(+) couples strongly to both accessory monomers, whereas the asymmetric state T(−) is more iso-

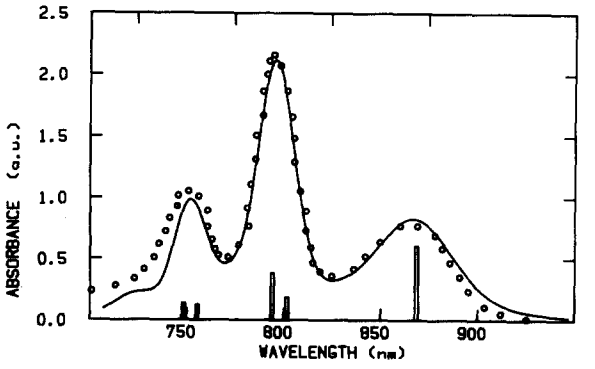

Fig. 1. Low-temperature (80 K) absorbance spectrum for *Rb. sphaeroides*. Experimental values (circles) from Ref. 10 are compared with model calculations (solid line). The bars show positions and intensities of the eigenstates.

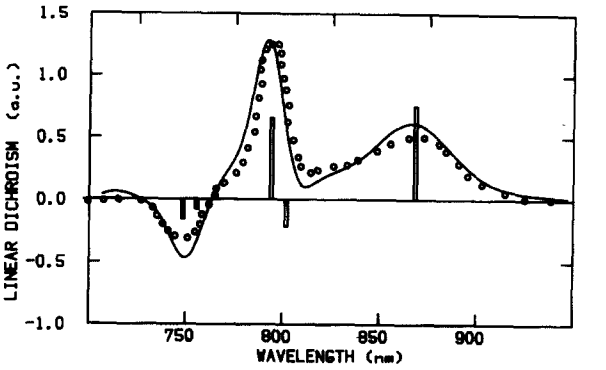

Fig. 2. Linear dichroism for *Rb. sphaeroides*. The circles show experimental data from Ref. 10. The solid line represents the model calculation. The bars indicate positions and intensities of the eigenstates.

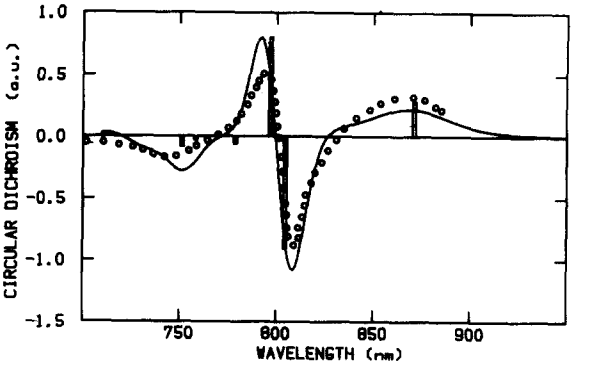

Fig. 3. Circular dichroism for *Rb. sphaeroides*. Experimental values from Ref. 11 are compared with model calculations (solid line). The bars show positions and intensities of the eigenstates.

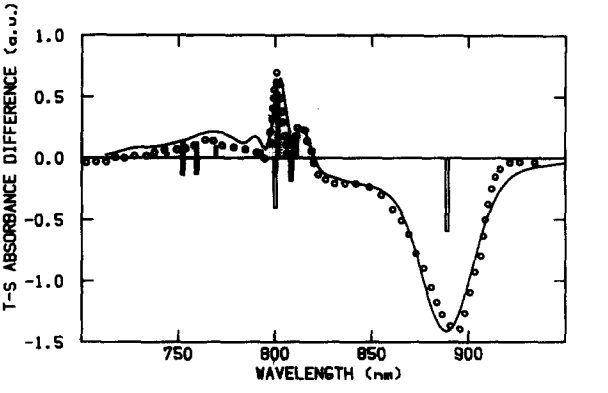

Fig. 4. Triplet-minus-singlet absorbance difference spectrum for *Rb. sphaeroides*. The calculated spectrum (solid line) is compared with the experimental T−S absorption difference spectrum from Ref. 13. Open (full) bars indicate positions and intensities of singlet (triplet) eigenstates.

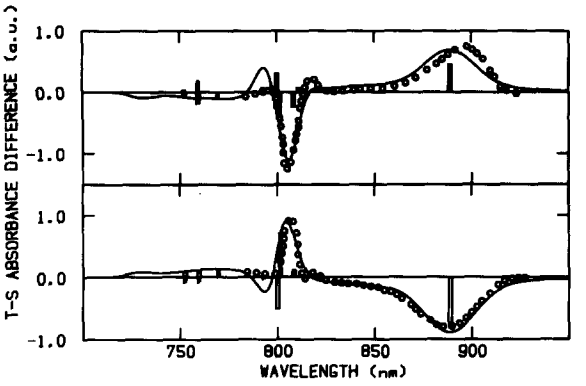

Fig. 5. Linear dichroic triplet minus singlet spectrum of *Rb. sphaeroides*. The polarization axis is parallel to the spin axis s_x (upper part) or to s_y (lower part). Solid lines show the calculated spectra. Open (full) bars show positions and intensities of the singlet (triplet) eigenstates.

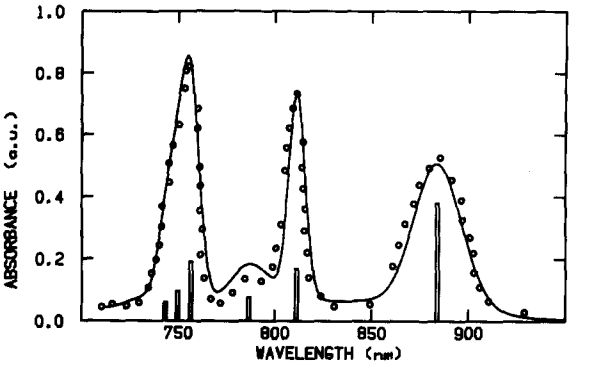

Fig. 6. Low-temperature (4 K) absorbance spectrum for *C. aurantiacus*. Experimental values (circles) from Ref. 3 are compared with model calculations (solid line). The bars show positions and intensities of the eigenstates.

lated. The higher state T(−) is broader than the other states. This could be explained by coupling to a broad distribution of T → T absorptions. The experimental data are simulated well if we assume partial delocalisation of the triplet with $(A^2 - B^2)/(A^2 + B^2)$ between 0 and 0.7 and $\alpha^2 - \beta^2$ between 0.3 and 0.9.

For the calculated linear dichroic T − S spectra (Fig. 5) we took angles between the polarisation of the dimer band and the spin axes of 90° and 5° and between the C_2-axis and the spin axes of 15° and 85°. These values agree with the data in the literature [13,14]. The agreement with the experimental data is quite good despite the missing correction for saturation effects of the experiments.

Results for *Chloroflexus aurantiacus*

In the reaction center of *C. aurantiacus* one accessory monomer is a pheophytin molecule. Therefore the spectra do not show the splitting of the monomer band as in the case of viridis and sphaeroides. Instead the absorption band of the pheophytins is much more pronounced. The experimental absorption spectrum [3] can be well reproduced (Fig. 6), assuming nearly degeneracy of all three pheophytins. The upper dimer band is clearly visible at 790 nm. Therefore the uncertainty in the value of the dimer coupling is much smaller than in the cases of viridis and sphaeroides. Our model calculations show much better agreement with the experiments if we assume that the extra pheophytin is located on the M-branch. If we put in on the L-branch, the absorbance band of the accessory monomer at 810 nm is reduced by a factor of 0.66, whereas the upper dimer band is increased by a factor of 1.3. From comparison with the experiments (Fig. 6) we conclude, that the pheophytin molecule has to be located on the M-branch.

The accuracy of the experimental LD spectrum is restricted, since it was calculated from the spectra of two samples containing different mixtures of reduced and oxidized reaction centers. Vasmel et al. [5] concluded that the polarization axis and the symmetry axis are nearly perpendicular and make an angle of 85°. Fig. 7 shows calculated (broken line) and experimental LD spectra. The highest exciton state, which is mainly the symmetric combination of the two pheophytins on the M-branch, has an appreciable positive LD, which is in disagreement with the experimental spectrum. This problem cannot be resolved by changing the polarization axis. However, agreement between experiment and model calculation is strongly improved if we assume that the Q_y transition of BP_{MA} is rotated by 12° in the molecular plane with respect to the corresponding transition of BC_{MA} for viridis. The full curve in Fig. 7 shows the calculation. The positive LD in the region of

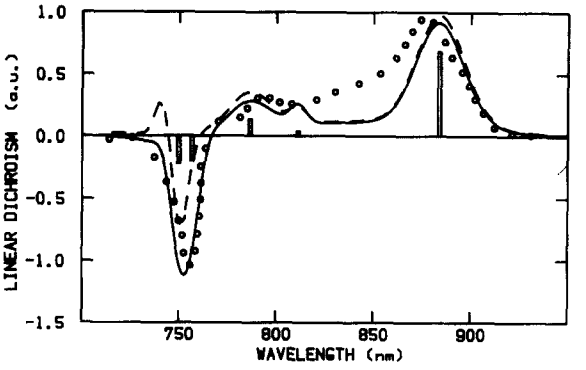

Fig. 7. Linear dichroism for *C. aurantiacus*. Experimental data (circles) from Ref. 3 are compared with model spectra (the broken line is calculated as for *Rps viridis*, whereas for the full line the transition dipole of BP_{mA} was rotated by 12° in the molecular plane). The polarization axis is parallel to the vector (−56, 0.59, 0.58) in the crystallographic coordinate system.

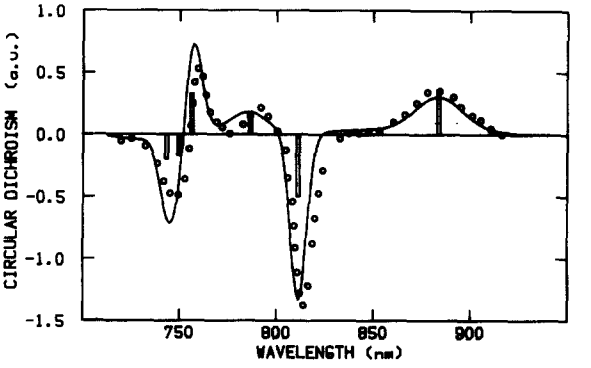

Fig. 9. Circular dichroism for *C. aurantiacus*. Experimental data (circles) from Ref. 3 and calculated spectrum (solid line) are shown. Bars indicate positions and intensities of the eigenstates.

the pheophytins disappears. Instead the accessory chlorophyll gains negative LD, which helps to fill the hole between the two dimer bands. The rotation of the BP_{MA} transition is also supported by photoselection experiments of Parot et al. [15], which measure the polarization of the chloroflexus absorption with respect to the lower dimer band. As Fig. 8 shows, the calculated polarization ratio agrees well with the experimental data (broken line). At the wavelength of the pheophytin absorption around 575 nm the agreement is even better if we take the rotated BP_{MA} transition (full line).

The calculated CD spectrum agrees very nicely with the experimental data (Fig. 9), even though these are taken at the higher temperature of 77 K.

For the angles between the spin axes and the lower dimer band we took 21° and 67°. These values are close to data in the literature 19° ± 3° and 65° ± 2° [4]. The charge-transfer contribution to the triplet state T is small as indicated by the large D value [8]. We took a value of 12%. The T − S absorption difference and its linear dichroism can be very well reproduced (Figs. 10 and 11)

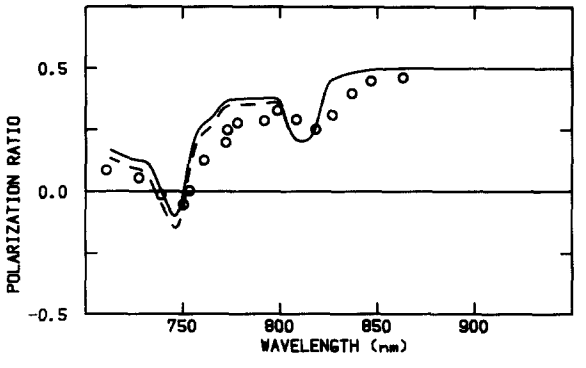

Fig. 8. Polarization ratio $(\Delta A_{\parallel} - \Delta A_{\perp})/(\Delta A_{\parallel} + \Delta A_{\perp})$ of the excitation spectrum for bleaching at 890 nm. Experimental data (circles) from Ref. 15 are compared with two different calculations (broken and full lines as in Fig. 7). The polarization axis is parallel to the transition dipole of the lower dimer band.

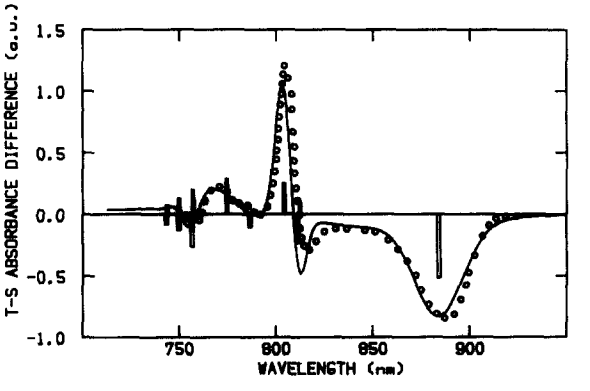

Fig. 10. Triplet-minus-singlet absorbance difference spectrum for *C. aurantiacus*. The calculated spectrum (solid line) is compared with the experimental T − S absorption difference spectrum from Ref. 4. Open (full) bars indicate positions and intensities of singlet (triplet) eigenstates.

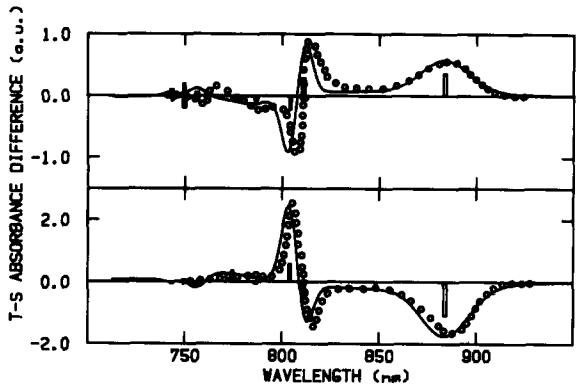

Fig. 11. Linear dichroic triplet-minus-singlet spectrum of *C. aurantiacus*. The polarization axis is parallel to the spin axis s_x (upper part) or to s_y (lower part). Solid lines show the calculated spectra. Open (full) bars show positions and intensities of calculated singlet (triplet) eigenstates. Circles show experimental data from Ref. 4.

if we assume an excited triplet state T(+) at a frequency position below the accessory monomer BC_{LA} and a much broader state T(−) between BC_{LA} and the pheophytins. This choice of parameters is quite similar to *Rps. viridis* and *Rb. sphaeroides*.

Again we have to assume delocalization of the triplet. The optimum value of $(A^2 - B^2)/(A^2 + B^2)$ between 0.8 and 1 suggests partial localisation of the triplet excitation on the pigment BC_{MP}. The excited triplet states T(±) seem to be stronger delocalized than T with an optimum value of $\alpha^2 - \beta^2$ between −0.3 and 0.

Earlier investigations [16] assumed that the triplet is localized on one special-pair pigment and the absorption at 807 nm is due to the other. This assumption differs from our model simulation, where the accessory monomer band is shifted to 805 nm and gains intensity as a result of its strong coupling to the delocalized triplet states of the dimer.

Summary and Discussion

The optical spectra of *Rb. sphaeroides* and *C. aurantiacus* can be well interpreted within the exciton model as applied earlier to *Rps. viridis* and using the same structure data. This points to the structural similarity of these three reaction centers.

For *C. aurantiacus* both dimer bands are apparent in the spectra. This allows a more precise determination of the special pair coupling of 680 cm^{-1} at 4 K. For *Rb. sphaeroides* the uncertainty is larger, but reasonable values are not too different from *C. aurantiacus*. The larger value of 1000 cm^{-1} we used for viridis is consistent with larger transition dipoles of the BChl *b* and pheophytin *b* molecules.

Introducing delocalized excited triplet states into the model, the T − S absorption difference and its LD can be interpreted consistently for all three reaction centers. These states couple to the excited states of the accessory monomers and pheophytins and provide an appropriate mechanism for the shifts and intensity redistribution of the accessory monomer bands.

Our analysis points to partial delocalisation of the triplet excitation over the special pair. This result, however, is based on the model calculation of transition dipoles and coupling constants for the triplet states (Eqn. 3). Possibly uncertainties could arise from unknown contributions of higher-excited triplet states or triplet charge-transfer states. The degree of triplet localization can be determined more accurately if the orientation of the spin axes is not just taken from experimental results, but also calculated within the model. Such an investigation has been performed very recently and will be published elsewhere [8].

Acknowledgements

The authors thank Dr. E.W. Knapp for many fruitful discussions and Dr. H. Vasmel for experimental information outlined in his thesis. This work was supported by the Deutsche Forschungsgemeinschaft (SFB 143).

References

1 Knapp, E.W., Scherer, P.O.J. and Fischer, S.F. (1986) Biochim. Biophys. Acta 852, 295–305
2 Deisenhofer, J., Epp, O., Miki, K., Huber, R. and Michel, H. (1984) J. Mol. Biol. 180, 385–398
3 Vasmel, H., Meiburg, R.F., Kramer, H.J.M., De Vos, L.J. and Amesz, J. (1983) Biochim. Biophys. Acta 724, 333–329
4 Vasmel, H. (1986) Doctoral thesis, University of Leiden
5 Vasmel, H., Amesz, J. and Hoff, A.J. (1986) Biochim. Biophys. Acta 852, 159–168
6 Connolly, J.S., Samuel, E.B. and Janzen, A.F. (1982) Photochem. Photobiol. 36, 565–574

7 Kooyman, R.P.H. and Schaafsma, T.J. (1980) J. Mol. Structure 60, 373–382
8 Scherer, P.O.J. and Fischer, S.F. (1986) Chem. Phys. Lett. 131, 153–159
9 Shuvalov, V.A., Amesz, J. and Duysens, L.N.M. (1986) Biochim. Biophys. Acta 851, 327–330
10 Rafferty, C.N. and R.K. Clayton (1978) Biochim. Biophys. Acta 502, 51–60
11 Shuvalov, v.A., Shkuropakov, A.Ya., Kulakova, S.M., Ismailov, M.A. and Shkuropakova, V.A. (1986) Biochim. Biophys. Acta 849, 337–346
12 Breton, J. (1985) Biochim. Biophys. Acta 810, 235–245
13 Hoff, A.J. (1985) in Encyclopedia of Plant Physiology (New Series), Vol. 19, Photosynthesis III (Stachelin, A.C. and Arntzen, C.J., eds.), Springer, Berlin
14 Hoff, A.J. (1985) in Antennas and Reaction Centers of Photosynthetic Bacteria (Michel-Beyerle, M.E., ed.), Series in Chemical Physics, Vol. 42, Springer, Berlin
15 Parot, P., Delmas, N., García, D. and Verméglio, A. (1985) Biochim. Biophys. Acta 809, 137–140
16 Den Blanken, H.J., Vasmel, H., Jongenelis, A.P.J.M., Hof, A.J. and Amesz, J. (1983) FEBS Lett. 161, 185–189